Ecotoxicology and Environmental Safety 169 (2019) 353–360

Contents lists available at ScienceDirect

Ecotoxicology and Environmental Safety

journal homepage: www.elsevier.com/locate/ecoenv

Insight into effects of citric acid on adsorption of phthalic acid esters (PAEs) in mangrove sediments

Haifeng Sun[a,b,c,*], Ruiyao Ma[a], Yanli Nan[a], Ruijie Feng[a]

[a] College of Environment and Resource, Shanxi University, Taiyuan 030006, China
[b] Department of Environmental Sciences, University of California, Riverside, CA 92521, USA
[c] Guangzhou Key Laboratory of Environmental Exposure and Health, School of Environment, Jinan University, Guangzhou 510632, China

ARTICLE INFO

Keywords:
Mangrove sediments
Citric acid
Phthalic acid esters
Adsorption
Particulate organic matter

ABSTRACT

The adsorption of phthalate esters (PAEs) in mangrove sediment greatly influences their availability to aquatic organisms, however, the adsorption processes of PAEs in mangrove sediment, as well as the effects of root exudates, are poorly understood. In this study, dimethyl phthalate (DMP), diethyl phthalate (DEP) and dibutyl phthalate (DBP) was used as model PAEs to determine the effects and mechanism of citric acid on the adsorption kinetics and isotherms of PAEs in the mangrove sediments. The adsorption kinetics followed pseudo-second order model, describing the characteristics of heterogeneous chemisorption of PAEs in mangrove sediments. The adsorption isotherms of DMP and DEP followed Freundlich model, implying the characteristics of surface multilayer heterogeneous adsorption; while the Henry model better described the adsorption isotherms of DBP, suggesting that hydrophobic partition accounted for DBP adsorption in the mangrove sediments. Inter-chemical variability was observed in adsorption capacity (q_e) with the sequence of DBP > DEP > DMP. Surface polarity index ((C-O + COOH + C=O)%) of particulate organic matter (POM) regulated the adsorption capacity of DMP and DEP in mangrove sediments, while different POM content among mangrove sediments explained the difference in the sorption strength for DBP. The presence of citric acid enhanced the q_e of the three PAEs by 6.4–12.6%. These findings are of great significance to reveal that the root exudates play a crucial role in the PAEs adsorption in mangrove sediments, and provide valuable information for availability of PAEs in mangrove ecosystem.

1. Introduction

Phthalate esters (PAEs) are ubiquitous in the environment due to their widespread usage in industrial, agricultural and domestic fields, including plastic products, pesticides, cosmetics and personal care products (Zeng et al., 2009; Cheng et al., 2013; Li et al., 2015). Statistically the worldwide production of PAEs exceeds five million tons annually (Maraqa et al., 2011; Sun et al., 2012), and accidently daily human consumption of PAEs may be as high as 70 μg kg^{-1} day^{-1} (Net et al., 2015). PAEs have a potential tendency for bioaccumulation and may act as endocrine disruption compounds (EDCs) affecting the normal function of the reproductive system and development of humans and animals at much low concentrations (Gu et al., 2005). For instance, several of the most common PAEs, such as dibutyl phthalate (DBP) and di-(2-ethylhexyl) phthalate (DEHP), are known to reduce the quality of human semen (Wu et al., 2018). Several regulatory bodies, including the US Environmental Protection Agency and the European Union, have classified PAEs as EDCs and as 'priority pollutants' (Sun et al., 2012).

Previous studies focused on the development of analytical methods (Lin et al., 2003), and distribution of individual congeners and commercial mixtures of PAEs in atmosphere and air particulate matter (Salapasidou et al., 2011; Chen et al., 2018), soil (Liu et al., 2010; Zhao et al., 2018), sewage sludge (Clarke and Smith, 2011), water and surface sediments (Fromme et al., 2002; Paluselli et al., 2018), and the tissues and fluids of wildlife and humans (Guo et al., 2011; Kim et al., 2011). Consequently, the contamination and environmental behaviors of PAEs have become an important research topic in the world. Due to the high hydrophobicity and low solubility of PAEs, most of them tend to be adsorbed on soil particles strongly, and the presence of soil organic matter (SOM) is of great importance for the adsorption of PAEs (Ahmed et al., 2015). Mangrove ecosystems, important intertidal estuarine wetlands along the coastlines of tropical and subtropical regions, are usually sinks of contaminants of emerging concern (CECs)

* Corresponding author at: College of Environment and Resource, Shanxi University, Taiyuan 030006, China.
E-mail address: hfsun86@sxu.edu.cn (H. Sun).

https://doi.org/10.1016/j.ecoenv.2018.11.034
Received 18 August 2018; Received in revised form 29 October 2018; Accepted 9 November 2018
Available online 17 November 2018
0147-6513/

from the aquatic system due to the high productivity and rich organic matters (Sun et al., 2016), and it plays an important role in the accumulation and bioconversion of CECs, including PAEs (Yuan et al., 2010), polybrominated diphenyl ether (Pan et al., 2017). Up to date, there is very limited information on the adsorption of PAEs by mangrove sediment.

Mangrove roots secrete a wide range of organic compounds into the rhizospheric environment, known as root exudates that are always divided into low- and high-molecular weight exudates (Haichar et al., 2014). Low-molecular-weight organic acids (LMWOAs) are chemically active, and they can be easily involved in a series of rhizospheric processes, such as the regulation of plant growth, detoxification of harmful elements (Tao et al., 2003; Lu et al., 2007), promoting the mobility of pyrene (An et al., 2010; Jia et al., 2018), and serving as substrates for microbial metabolism (Shukla et al., 2011). However, the fate appertaining to the adsorption behavior of PAEs in mangrove sediments affected by LMWOAs remains unclear.

The range of LMWOAs secreted by roots varies with plant species (Wang et al., 2014), but citric, lactic and acetic acids are most frequently detected and dominant components of LMWOAs in mangrove sediments (Lu et al., 2007). Therefore in the present study, citric acid was selected as model LMWOAs, and the objective was to investigate the effects of citric acid on the adsorption of dimethyl phthalate (DMP), diethyl phthalate (DEP) and dibutyl phthalate (DBP) by mangrove sediments.

2. Materials and methods

2.1. Chemicals and sediment

DMP (purity > 99.5%), DEP (purity > 99.5%) and DBP (purity > 99%) were purchased from Dr. Ehrenstorfer GmbH (Augsburg, Germany). The characteristics of the three main compounds were depicted in Table S1. NaN_3, $CaCl_2$, methanol and citric acid with the purity of analytical grade were obtained from Sinopharm Chemical Reagent Co., Ltd. (Shanghai, China).

The sediment samples were collected from the surface layer (0–20 cm) of Yunxiao mangrove swamp (23°58′N, 117°27′E), Jiulongjiang Estuary mangrove wetland (24°21′N, 117°54′E) in Fujian province (China), and Zhanjiang Estuary mangrove wetland (20°72′N, 110°25′E) in Guangzhou province (China), respectively. The sediment samples were labeled as JL, YX and ZJ mangrove sediments, respectively. The sediment samples were air-dried, homogenized and passed through 2-mm mesh prior to be used for adsorption experiments. For comprehensively understanding the role of particulate organic matter (POM) in PAEs adsorption, mangrove sediments with low mineral content was prepared using the chemical extraction method (Lopez-Sangil and Rovira, 2013).

2.2. Characteristics of mangrove sediments

The organic carbon content of the sediment samples were measured using a Total Organic Carbon Analyzer (TOC-5000, Shimadzu, Japan). According to the method recorded in pervious study (Lopez-Sangil and Rovira, 2013), free/occluded POM and mineral-associated organic matter fractions were separated from the mangrove sediment samples. A Vario El Cube Elemental Analyzer (Elementar, Germany) was applied for the CHON analysis of POM. The mineral distribution in mangrove sediments was measured using Field Emission Scanning Electron Microscopy equipped with Energy Dispersive X-ray spectroscopy (FESEM-EDX) at 25 kV (LEO 1530, UK). The C assignments of ^{13}C NMR spectra were obtained using a Bruker Avance III 600 MHz NMR spectrometer (Germany) at a ^{13}C frequency of 100 MHz. The compositions of different carbon types were obtained via scanning six regions, including alkyl C (0–50 ppm), O-alkyl C (50–109 ppm), aromatic C (109–145 ppm), phenolic C (145–163 ppm), carboxyl C (163–190 ppm) and carbonyl C (190–220 ppm). The surface functionalities were determined using a Quantum 2000 Scanning Electron Microprobe (Physical Electronics, US) combined with X-ray Photoelectron Spectroscopy (XPS) (225 W, 15 mA, 15 kV) (EscaLab 250Xi, Thermo Scientific, US).

2.3. Adsorption experiment

Batch experiments were performed to examine the effects of citric acid on adsorption kinetics and isotherms of DMP, DEP and DBP in the sediment-water system as described in previous studies (Sun et al., 2011; Wu et al., 2018). Background solutions contained 100 mg L^{-1} NaN_3 to inhibit bacterial growth, and 0.01 M $CaCl_2$ to maintain a constant ionic strength (Sun et al., 2012). The stock solutions of solutes dissolved in methanol were diluted using ultrapure water to obtain the working solutions containing different solute concentrations (0.1–200 mg L^{-1} for DMP, 0.1–120 mg L^{-1} for DEP and 0.1–8 mg L^{-1} for DBP). 50 mg of sediment samples were treated with 50 mL citric acid (50 mg L^{-1}) in a 20-mL brown glass bottle. Methanol concentration in aqueous phase was controlled below 0.1% to avoid the co-solvent effect. The ratio of solid/liquid was obtained prior to the experiment to achieve 20–80% adsorption of initial adsorbates at equilibrium. All the bottles were incubated at 30 rpm and 25 °C in the dark for 0.05, 0.5, 2, 5, 10, 15 and 20 h. At each time point, three replicates were performed for PAEs analyses. Blanks with no additional sorbents showed that the losses caused by the adsorption to bottle wall and degradation were found to be less than 3% of the spiked PAEs content.

2.4. PAEs analysis

The instrumental analysis for the DMP, DEP and DBP were performed according to the method recorded in previous study (Wu et al., 2018). 2 mL samples were first centrifuged at 10,000 rpm for 3 min. The concentrations of DMP, DEP and DBP in supernatant were analyzed using HPLC (Agilent 1100, reversed phase C18, 250 mm × 4.6 mm × 5 μm) with UV detection. The mobile phase consisted a mixture of methanol and ultra-pure water (80:20, v/v) at a flow rate of 0.8 mL min^{-1}. The injection volume and column temperature was 20 μL and 35 °C, respectively. The detection wavelength of the UV detector was set at 226 nm.

2.5. Data analysis

2.5.1. Adsorption kinetics

The adsorption kinetics of the three PAEs in sediment in the absence and presence of citric acid were described using the pseudo-first-order (Eq. (1)) and pseudo-second-order models (Eq. (2)) (Wu et al., 2018).

$$\ln\left(\frac{q_e}{q_e - q_t}\right) = \ln q_e + k_1 t \quad (1)$$

$$\frac{t}{q_t} = \frac{1}{k_2 q_e^2} + \frac{t}{q_e} \quad (2)$$

where q_e and q_t (mg kg^{-1}) represent the amounts of adsorbed PAEs at equilibrium and at any time t (h), respectively; k_1 (h^{-1}) and k_2 (kg (mg $h)^{-1}$) are the rate constants of the pseudo-first-order and pseudo-second-order equations, respectively.

2.5.2. Adsorption isotherms

The adsorption isotherms of PAEs in mangrove sediments with and without citric acid were described using Henry (Eq. (3)), Langmuir (Eq. (4)) and Freundlich models (Eq. (5)) (Réguer et al., 2011):

$$q_e = k_H C_e \quad (3)$$

$$\frac{1}{q_e} = \frac{1}{q_m k_L C_e} + \frac{1}{q_m} \quad (4)$$

$$q_e = k_F C_e^{1/n} \quad (5)$$

where q_e (mg kg^{-1}) is the concentration of PAEs adsorbed by the sediment; C_e (mg L^{-1}) denotes the equilibrium concentration of PAEs in the solution phase; k_H (L mg^{-1}) represent the Henry model adsorption coefficient (partition coefficient between sediment and water); k_L (L mg^{-1}) denotes the Langmuir model coefficient as related to t the adsorption intensity and affinity, and q_m (mg kg^{-1}) is the maximum adsorption capacity of PAEs; k_F ((mg kg^{-1})/(mg L^{-1})^n) refers to the binding energy constant reflected the adsorption capacity of PAEs to adsorbents and n represents the isotherm nonlinearity index ($0 < n < 1$).

The thermodynamic parameter of Gibbs free energy (ΔG) was calculated through the following equation (Vimonses et al., 2009):

$$\Delta G = -RTlnk_H$$

where T = 298.15 K; R is constant (8.314 J (mol K)$^{-1}$), T is the absolute temperature in Kelvin (K), k_H denotes the Henry coefficient (L mg^{-1}).

2.6. Statistical analysis

All experiments were performed in triplicate and the average values were presented as the final results. The statistical analysis of variance (ANOVA) was applied with SPSS (version 19.0) at significance level of 95% ($P < 0.05$).

3. Results and discussions

3.1. Adsorption kinetics of PAEs in mangrove sediments

The adsorption kinetics of DMP, DEP and DBP in mangrove sediments are depicted Fig. 1. The adsorption processes could be divided into two stages, regardless of the presence of citric acid. The initial step was fast and lasted approximately 2 h. During this stage, the adsorbed amount of PAEs in mangrove sediments increased sharply. In the second step, the increase in adsorption amount became slower. Finally, no significant change was observed in the adsorption amount of PAEs in the sediments over time, indicating that the adsorption achieved equilibrium. Overall, all of the three PAEs reached a final equilibrium within 10 h. For each PAE chemical, the maximum adsorption capacities (q_e) with citric acid were greater than that without citric acid, indicating that the addition of citric acid promoted the PAEs adsorption.

In this study, the mechanism explaining the adsorption processes of PAEs in mangrove sediments was studied by fitting adsorption kinetics to pseudo-first-order and pseudo-second-order models. As recorded previously (Mirmohamadsadeghi et al., 2012; Wu et al., 2018), pseudo-first-order model describes the single layer of adsorption through boundary layer diffusion, while pseudo-second-order model assumes that the chemisorption is the rate-limiting step. The fitting results and related parameters for PAEs adsorption in mangrove sediments using the two models were displayed in Fig. 1 and Table 1, respectively. Obviously, the pseudo-second-order model gave better fit for the adsorption kinetics of three PAEs in mangrove sediments as suggested by their higher correlation coefficients (R^2) than that of pseudo-first-order model, regardless of the presence of citric acid. The observation indicates the chemisorption of PAEs in mangrove sediments, including by the valence electron forces through sharing or exchanging electrons between the active groups on sediment surfaces and PAEs (Wang et al., 2016). For any given mangrove sediment, the pseudo-second-order adsorption rate constants (k_2) followed DBP > DEP > DMP (Table 1), which was in good agreement with the adsorption rate of PAEs to the clay layer (Liu et al., 2013). Linear relationship was found between k_2 and the straight chain carbon number of PAEs (Fig. 2). Specifically, the equations were as follows for the sediments without citric acid: YX, $k_2 = 0.075 + 0.22\ n_{SC}$ ($R^2 = 0.99$); JL, $k_2 = 0.048 + 0.27\ n_{SC}$ ($R^2 = 0.98$); ZJ, $k_2 = 0.056 + 0.19\ n_{SC}$ ($R^2 = 0.99$). Meanwhile, the equations were as follows for the ones with citric acid: YX, $k_2 = 0.076 + 0.27\ n_{SC}$ ($R^2 = 0.98$); JL, $k_2 = 0.041 + 0.33\ n_{SC}$ ($R^2 = 0.99$); ZJ, $k_2 = 0.044 + 0.28\ n_{SC}$ ($R^2 = 0.99$).

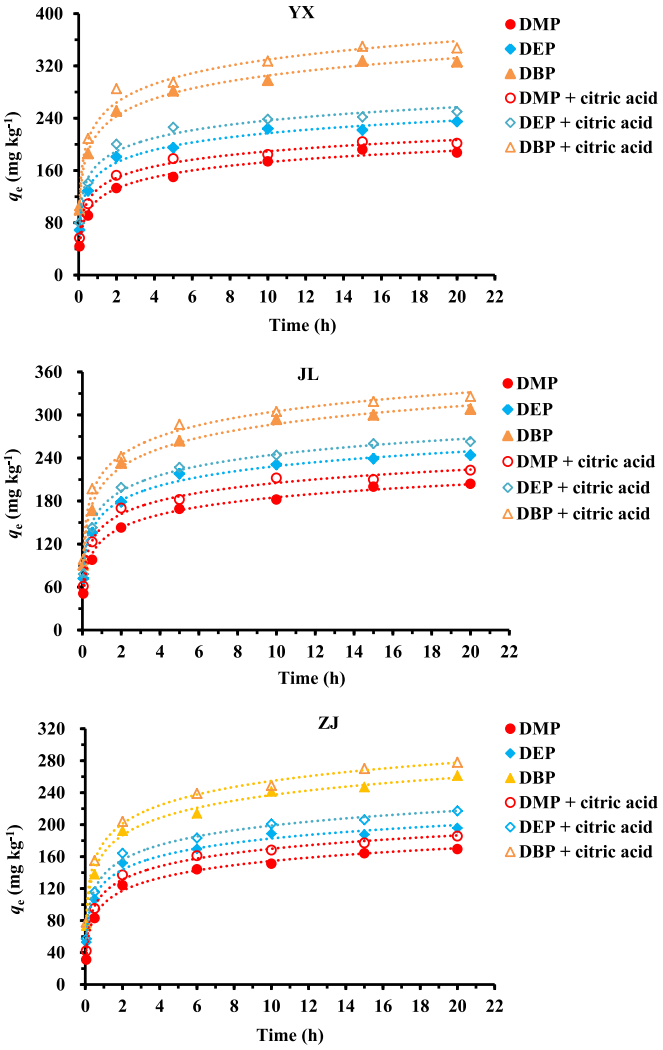

Fig. 1. Adsorption kinetics of DMP, DEP and DBP in mangrove sediments (solid marks) with simulations of pseudo-second-order model, as affected by 50 mg L^{-1} citric acid (hollow marks).

The q_e of the three PAEs varied significantly following the sequence of DBP > DEP > DMP ($P < 0.05$), regardless of the presence of citric acid (Fig. 1 and Table 1), indicating the q_e value escalated with the increasing straight chain carbon number of PAEs, or adsorbed concentrations were positively proportional to PAE hydrophobicity, with strongest sorption for the highly nonpolar DBP followed by the polar DEP and DMP. The result was consistent with the adsorption of PAEs in the clay layer reported by Liu et al. (2013), specifically, partition coefficient increased with carbon numbers of the straight carbon chain. In addition, the q_e varied with mangrove sediments of different sources, following JL > YX > ZJ for DMP and DEP, and following YX > JL > ZJ for DBP. The adsorption capacity for organic contaminants has been reported to be greatly dependent on organic matter of soils/sediments (Cornelissen et al., 2005; Xu and Li, 2008). Wu et al. (2018) found a significant positive correlation between adsorption capacity of DBP and SOM content in soil. Different from previous studies, no significant correlation between q_e and the total organic matter (TOM) were observed for the spiked mangrove sediments in this work. Recently, Cao et al. (2015) reported that the sorption capacity of POM for polycyclic aromatic hydrocarbons (PAHs) is much higher than that of the SOM-

Table 1
Fitting results of adsorption kinetics of PAEs in mangrove sediments using pseudo-first-order and pseudo-second-order models.

PAEs	$q_{e,exp}$ (mg kg^{-1})			pseudo-first-order model							
				$q_{e,calc}$ (mg kg^{-1})			k_1			R^2	
	YX	JL	ZJ	YX	JL	ZJ	YX	JL	ZJ	YX	JL
DMP	187.4 ± 3.8	204.9 ± 8.2	169.3 ± 2.9	165.7 ± 5.5	183.6 ± 6.9	147.2 ± 4.6	28.8 ± 4.1	35.9 ± 8.4	33.7 ± 7.0	0.88	0.93
DMP + CA	201.6 ± 6.2	223.7 ± 3.7	185.5 ± 3.1	179.4 ± 7.9	204.8 ± 8.4	164.4 ± 5.8	34.6 ± 9.6	42.6 ± 4.8	36.5 ± 6.5	0.91	0.92
DEP	225.0 ± 4.4	244.6 ± 6.0	195.7 ± 5.2	213.5 ± 4.8	224.5 ± 5.6	173.8 ± 7.3	36.5 ± 9.1	40.1 ± 8.3	34.8 ± 6.0	0.85	0.89
DEP + CA	240.1 ± 5.7	263.8 ± 5.4	217.1 ± 7.0	228.7 ± 6.1	242.6 ± 4.5	195.5 ± 3.9	38.1 ± 7.5	44.2 ± 6.8	40.3 ± 4.6	0.90	0.91
DBP	326.3 ± 4.1	302.5 ± 7.1	261.3 ± 4.8	304.8 ± 7.5	286.4 ± 5.8	239.0 ± 6.8	59.8 ± 9.2	45.4 ± 7.5	37.9 ± 8.9	0.92	0.90
DBP + CA	367.5 ± 3.5	326.6 ± 5.3	277.9 ± 2.6	327.0 ± 9.2	305.2 ± 7.7	258.6 ± 5.1	59.7 ± 7.4	55.7 ± 8.8	48.1 ± 5.8	0.94	0.93

PAEs	pseudo-first-order model	pseudo-second-order model								
	R^2	$q_{e,calc}$ (mg kg^{-1})			k_2			R^2		
	ZJ	YX	JL	ZJ	YX	JL	ZJ	YX	JL	ZJ
DMP	0.87	170.5 ± 4.7	189.2 ± 5.2	152.9 ± 3.8	0.28 ± 0.01	0.33 ± 0.02	0.25 ± 0.03	0.96	0.99	0.98
DMP + CA	0.94	184.2 ± 5.6	208.6 ± 6.6	170.1 ± 4.3	0.34 ± 0.01	0.37 ± 0.01	0.32 ± 0.02	0.98	0.96	0.99
DEP	0.92	218.6 ± 3.9	229.4 ± 4.7	178.5 ± 6.2	0.38 ± 0.02	0.36 ± 0.01	0.31 ± 0.02	0.97	0.97	0.98
DEP + CA	0.89	233.0 ± 4.5	247.7 ± 3.1	200.4 ± 2.5	0.43 ± 0.01	0.41 ± 0.02	0.36 ± 0.01	0.98	0.99	0.95
DBP	0.93	310.8 ± 5.0	292.5 ± 4.8	244.6 ± 5.3	0.51 ± 0.03	0.47 ± 0.02	0.42 ± 0.02	0.96	0.99	0.99
DBP + CA	0.90	332.7 ± 6.4	310.8 ± 5.9	263.7 ± 4.0	0.57 ± 0.01			0.99	0.98	0.97

Where CA represents citric acid of 50 mg L^{-1}; $q_{e,exp}$ (mg kg^{-1}) is adsorbate concentrations in the mangrove sediments at adsorption equilibrium of PAEs; $q_{e,calc}$ (mg kg^{-1}) is the total solid concentrations of DBP at apparent equilibrium obtained from pseudo-first-order and pseudo-second-order models; k_1 (h^{-1}), k_2 (kg (mg h)$^{-1}$) are the rate constants of pseudo-first-order and pseudo-second-order models, respectively.

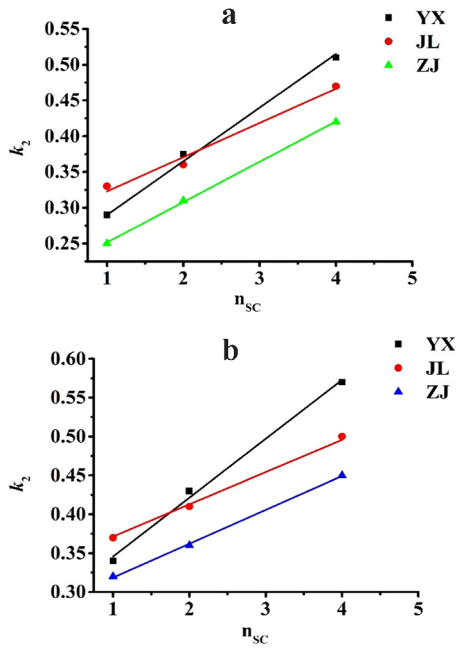

Fig. 2. Relationship of k_2 with the straight chain carbon numbers of PAEs (n_{sc}) for the mangrove sediments in absence of citric acid (a) and in presence of citric acid (b).

mineral systems, and the adsorbed PAHs tended to reside in POM phase in mangrove sediments. SEM-EDX data (Fig. S1) showed that the content of mineral cations, including Al^{3+}, Fe^{3+}, Mg^{2+} and Ca^{2+}, in the mangrove sediments decreased prominently after the chemical extraction treatment, indicating that the original form of the SOM-mineral system changed to POM (Rinklebe et al., 2015). However, in this study, no good correction was found between q_e and the POM content for DMP and DEP, except for DBP. From Table 1 and S2, YX with the highest POM content had the maximum q_e values for DBP, but had medium q_e values for DMP and DEP; JL with medium POM content had the highest q_e values for DMP and DEP, but had medium q_e values; ZJ with the least POM content had the lowest q_e values for the three PAEs. Consequently, these results suggests that the q_e of mangrove sediments for the three PAEs not just displayed a POM-dependent response, and there are other contributing factors to influence the adsorption capacity of sediments for PAE chemicals.

For further providing more information about the adsorption mechanism, adsorption kinetics of the three PAEs was further examined using intra-particle diffusion model (Wu et al., 2018). For instance, the fitting curves were divided into two-linear plots for the adsorption of DMP in YX mangrove sediment (Fig. S2), suggesting a two-step adsorption process. In the initial stage, rapid boundary layer diffusion of PAEs on the external sediment surface occurred around 2 h through liquid film diffusion. During the second stage, pore diffusion or intra-particle diffusion was the dominant process. Finally, the adsorption of three PAEs in mangrove sediment achieved equilibrium. Similar results were also observed for JL and ZJ mangrove sediments (data not shown). Therefore, regardless of the presence of citric acid, both intra-particle diffusion and external mass transfer played a vital role in regulating the adsorption of PAEs.

3.2. Adsorption isotherms of PAEs in mangrove sediments

The adsorption isotherms of the three PAEs in mangrove sediments were analyzed using the Henry, Freundlich and Langmuir models. The results are shown in Fig. 3 and Table 2 and 3. For DMP and DEP, the R^2 values of the Freundlich model (0.97–0.99) was basically higher than the Henry (0.93–0.97) and Langmuir models (0.88–0.92), indicating

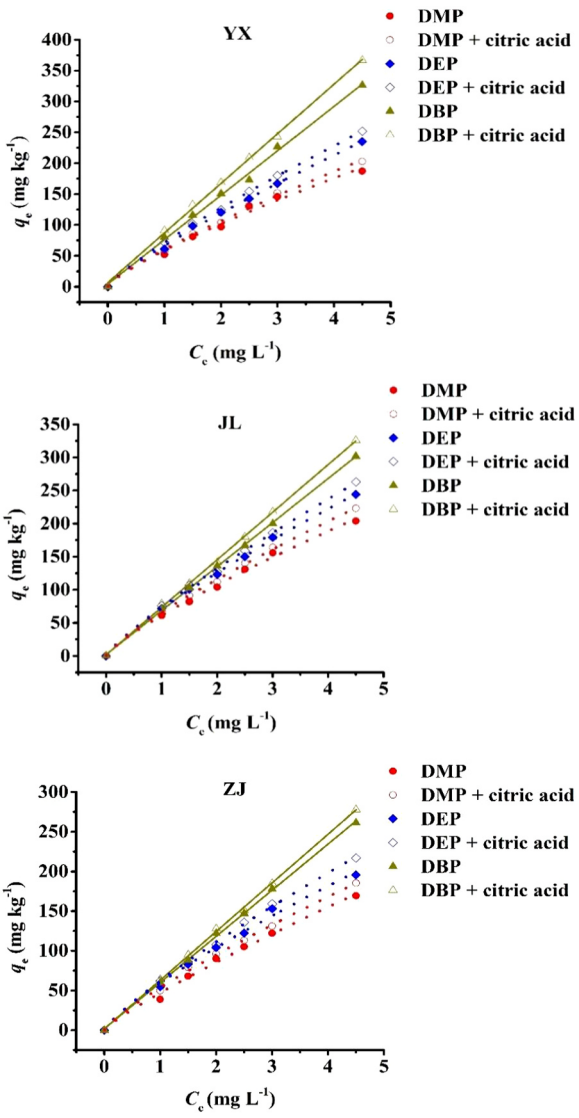

Fig. 3. Adsorption isotherms of PAEs in mangrove sediments (solid marks) as affected by 50 mg L^{-1} citric acid (hollow marks). Henry model (line), Freundlich model (dotted line).

that Freundlich model was more suitable than the other two models to describe the adsorption isotherms of DMP and DEP in mangrove sediments. This suggests that the adsorption of DMP and DEP in sediments was regulated by the surface multilayer heterogeneous adsorption, rather than the hydrophobic partition and the single-layer adsorption on the smooth and uniform surface (Lin et al., 2018). But for DBP, the adsorption isotherm data fitted better into Henry model (R^2 = 0.98–1.00) than both Freundlich (R^2 = 0.93–0.97) and Langmuir (R^2 = 0.87–0.91) models, revealing that the hydrophobic partition regulated the DBP adsorption.

As the increment of PAEs concentrations, the presence of citric acid increased the k_F values markedly for the three kinds of sediments (Table 2 and 3). For instance, the k_F values of DMP were (70.5 ± 2.7) (mg kg^{-1})/(mg L^{-1})^n in JL mangrove sediment with the addition of 50 mmol L^{-1} citric acid, which increased by 19.6% as compared to the corresponding controls (61.3 ± 1.9) (mg kg^{-1})/(mg L^{-1})^n. Similar results were also observed for the other two PAEs and mangrove sediments. On the one hand, the presence of citric acid increased the POM content in TOM by 6.4–8.6% mainly via enlarging the proportion of aromatic, carboxyl or carbonyl C in the three mangrove sediments (Table S2). On the other hand, citric acid also increased the proportion

Table 2
Fitting results of adsorption isotherms of PAEs in mangrove sediments using different models.

Sediments	Henry model		Freundlich model			Langmuir model			
	k_H (L mg^{-1})	R^2	k_F (mg kg^{-1})/(mg L^{-1})^n	n	R^2	k_L (L mg^{-1})	q_m (mg kg^{-1})	R^2	ΔG (kJ mol^{-1})
DMP									
YX	39.2 ± 2.5	0.94	45.9 ± 2.4	1.22 ± 0.04	0.99	4.7 ± 0.2	220.6 ± 6.4	0.92	− 8.4 ± 0.4
JL	45.8 ± 1.4	0.96	61.3 ± 1.9	1.17 ± 0.06	0.98	3.6 ± 0.1	285.1 ± 5.7	0.89	− 9.6 ± 0.7
ZJ	32.7 ± 1.0	0.93	39.8 ± 1.7	1.06 ± 0.03	0.98	2.4 ± 0.2	147.0 ± 3.5	0.91	− 10.5 ± 0.9
DEP									224.5 ± 5.6
YX	44.6 ± 1.8	0.95	52.6 ± 1.5	1.30 ± 0.02	0.98	5.8 ± 0.3	279.6 ± 7.2	0.92	− 10.2 ± 1.2
JL	56.3 ± 2.1	0.93	61.4 ± 1.8	1.25 ± 0.03	0.99	4.4 ± 0.4	358.5 ± 4.8	0.90	− 8.5 ± 0.6
ZJ	40.5 ± 1.6	0.94	47.0 ± 1.7	1.03 ± 0.05	0.99	3.7 ± 0.2	211.4 ± 5.3	0.93	− 9.1 ± 0.5
DBP									
YX	72.4 ± 1.9	0.98	75.2 ± 2.2	1.17 ± 0.04	0.96	7.3 ± 0.6	400.8 ± 6.9	0.87	− 9.7 ± 1.0
JL	67.1 ± 0.8	0.99	71.3 ± 2.0	1.09 ± 0.07	0.97	6.5 ± 0.4	384.5 ± 4.6	0.90	− 10.4 ± 0.4
ZJ	58.4 ± 1.3	0.98	59.8 ± 1.5	1.04 ± 0.02	0.94	4.2 ± 0.3	362.1 ± 7.0	0.89	− 8.3 ± 0.6

Where k_H (L mg^{-1}) denotes the adsorption coefficient of Henry model; k_F ((mg kg^{-1})/(mg L^{-1})^n) is the Freundlich adsorption affinity-related coefficient, and n represents the correction exponent; k_L (L mg^{-1}) represents the Langmuir constant as related to the adsorption binding energy of the adsorbent, and q_m (mg kg^{-1}) denotes the theoretical maximum adsorption capacity of PAEs; ΔG is the thermodynamic parameter of Gibbs free energy.

of some surface functionalities (COOH, C=O) in POM of sediments (Table S3). As reported, organic materials act as the main sorption sites for organic contaminants (Xu and Li, 2008). Consequently, the availability of PAEs in the mangrove sediments decreased or the adsorption capacity increased. Additionally, the addition of citric acid decreased the *n* values, implying stronger linearity of isothermal adsorption, the inhibition of the multilayer heterogeneous adsorption and promotion of hydrophobic partition of PAEs to mangrove sediments. Regardless of the presence of citric acid, all the thermodynamic parameter of Gibbs free energy (ΔG) values were lower than zero (Table 2 and 3), indicating that the adsorption of PAEs might be spontaneous and predominated by passive process (Vimonses et al., 2009).

3.3. Organic precursor materials responsible for adsorption of PAEs

The existing literatures have reported that the adsorption strength of adsorbent for sorbates is related to the polarity organic matter components, alkyl carbon content and intermolecular hydrogen bond interactions, etc. (Sun et al., 2012; Wu et al., 2018). To further determine the interactions between PAEs, mangrove sediments and citric acid, the bulk and surface chemical compositions of sediments were examined using solid state ^{13}C NMR and XPS (Tables S2 and S3). As mentioned above, no significant correlation between the q_e and TOM was observed for the spiked mangrove sediments. The ^{13}C NMR spectroscopy showed that the POM values were 41.6, 36.1 and 29.5 g kg^{-1} for mangrove sediments YX, JL and ZJ without citric acid, respectively, while 45.2, 38.4 and 31.7 g kg^{-1} for YX, JL and ZJ with citric acid (Table S2). The q_e values of DBP exhibited linear relationship with the POM content in TOM (Fig. 4), indicating hydrophobic partitioning into POM dominated the adsorption of DBP into mangrove sediments, which might be largely attributed to the fact that the crystalline structure of POM limited the role of the bulk composition in the adsorption of DBP. This was further supported by the result of adsorption isotherms that highlighted the hydrophobic partition into POM as an important component for the adsorption of DBP. However, no strong correlation was observed between q_e and the POM content for DMP and DEP, implying that there might be additional adsorption mechanisms in place.

Surface polarity index of the sorbents is approximated by the sum of the relative proportions (%) of O-containing functional groups (C-O + COOH + C=O) from XPS analysis (Table S3). Notably, a significant difference was observed in the surfaces polarity of the mangrove sediments ($P < 0.05$), following JL (34.7%) > YX (31.2%) > ZJ (27.8%) without citric acid treatment, and JL (36.8%) > YX (32.7%) > ZJ (29.3%) with citric acid. This suggests that the presence of citric acid enhanced the surface polarity of mangrove sediments, which could be explained by the fact that the addition of citric acid increased the

Table 3
Fitting results of adsorption isotherms of PAEs in mangrove sediments in the presence of citric acid using different models.

Sediments	Henry model		Freundlich model			Langmuir model			
	k_H (L mg^{-1})	R^2	k_F (mg kg^{-1})/(mg L^{-1})^n	n	R^2	k_L (L mg^{-1})	q_m (mg kg^{-1})	R^2	ΔG (kJ mol^{-1})
DMP									
YX	44.7 ± 1.8	0.96	50.9 ± 3.0	1.14 ± 0.03	0.97	2.8 ± 0.2	452.7 ± 3.9	0.91	− 8.7 ± 0.6
JL	51.8 ± 2.5	0.97	70.5 ± 2.7	1.08 ± 0.04	0.98	3.5 ± 0.3	571.4 ± 4.5	0.89	− 10.1 ± 0.3
ZJ	42.3 ± 1.6	0.96	47.0 ± 1.6	1.03 ± 0.02	0.98	2.1 ± 0.1	313.2 ± 2.8	0.91	− 10.8 ± 0.5
DEP									
YX	59.6 ± 3.2	0.97	62.5 ± 1.4	1.19 ± 0.05	0.98	3.7 ± 0.4	511.4 ± 5.6	0.90	− 10.4 ± 1.0
JL	62.7 ± 2.5	0.94	68.7 ± 3.1	1.16 ± 0.02	0.99	5.2 ± 0.2	480.5 ± 6.0	0.88	− 8.9 ± 0.4
ZJ	48.2 ± 1.9	0.96	53.6 ± 2.8	1.02 ± 0.04	0.97	2.9 ± 0.1	389.3 ± 3.7	0.91	− 9.4 ± 0.2
DBP									
YX	81.5 ± 2.3	0.99	83.9 ± 2.5	1.05 ± 0.02	0.96	6.8 ± 0.5	755.4 ± 4.8	0.89	− 10.5 ± 1.3
JL	72.4 ± 1.4	1.00	78.3 ± 3.6	1.03 ± 0.05	0.93	5.6 ± 0.6	726.8 ± 5.1	0.91	− 10.9 ± 0.7
ZJ	61.7 ± 1.8	0.99	71.7 ± 1.9	1.00 ± 0.04	0.95	3.5 ± 0.2	610.3 ± 6.4	0.88	− 9.0 ± 0.5

Where k_H (L mg^{-1}) denotes the adsorption coefficient of Henry model; k_F ((mg kg^{-1})/(mg L^{-1})^n) is the Freundlich adsorption affinity-related coefficient, and n represents the correction exponent; k_L (L mg^{-1}) represents the Langmuir constant as related to the adsorption binding energy of the adsorbent, and q_m (mg kg^{-1}) denotes the theoretical maximum adsorption capacity of PAEs; ΔG is the thermodynamic parameter of Gibbs free energy.

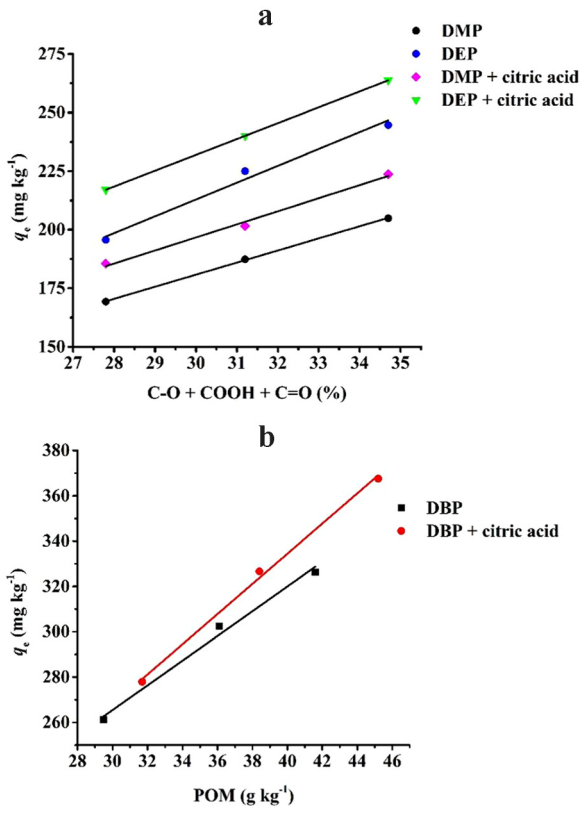

Fig. 4. The correlation between q_e and the surface polarity index (a) of POM, POM content (b) in mangrove sediments without and with the treatment of 50 mg L^{-1} citric acid.

proportion of O-containing functional groups (COOH, C=O) in POM of mangrove sediments (Table S3). It was interesting to note that the q_e values of DMP and DEP exhibited significantly linear relationships with the surface polarity of mangrove sediments (Fig. 4). According to Zhang et al. (2008), the O atom of the PAEs-containing ester group, as hydrogen (H)-bonding acceptor,

can form H- bonds with H-donating functional groups on sorbents. The O atom of carbonyl or carboxyl groups in aromatic structures might also act as H-bonding acceptor sites and form hydrogen bonding with the oxygen atom of the ester group of DMP and DEP through bridging water molecules. Therefore, the variability of surface polarity explained the difference in sorbent strength to relatively polar DMP and DEP among the three mangrove sediments.

4. Conclusions

Firstly, this work illustrated the adsorption kinetics of DMP, DEP and DBP in the mangrove sediment-water systems that could be well described using the pseudo-second-order model, regardless of the presence of citric acid, revealing the characteristics of heterogeneous chemisorption. Secondly, inter-chemical variability occurred in the adsorption isotherms of the three PAEs and dominant mechanism for sorption strength. Specifically, the adsorption isotherms of DMP and DEP followed the Freundlich model and surface polarity index of POM explained the difference in the adsorption capacity for DMP and DEP among the three mangrove sediments; in contrast, the Henry model fitted well into the adsorption isotherms of DBP, and POM content in TOM dominated the adsorption ability of mangrove sediments for DBP. Citric acid promoted DBP adsorption mainly via the enhancement of hydrophobic partition, but enhanced DMP and DEP adsorption by increasing both the adsorption sites and surface polarity index on the sediment surfaces. Therefore, LMWOAs played a crucial role in affecting the transport of PAEs in mangrove sediment.

Acknowledgments

The authors would like to thank the financial support from the National Natural Science Foundation of China (Nos. 21507077 and 91543203), Key Laboratory of Soil Environment and Nutrient Resources of Shanxi Province, China (2017001), the State Scholarship Fund of China Scholarship Council (File No. 201708140010), Guangzhou Key Laboratory of Environmental Exposure and Health, China (No. GZKLEEH201609), and Grant from the Central Promotion Plan of Talent Development, China (rsc1148).

Appendix A. Supporting information

Supplementary data associated with this article can be found in the online version at doi:10.1016/j.ecoenv.2018.11.034.

References

Ahmed, A.A., Thiele-Bruhn, S., Aziz, S.G., Hilal, R.H., Elroby, S.A., Al-Youbi, A.O., Leinweber, P., Kühn, O., 2015. Interaction of polar and nonpolar organic pollutants with soil organic matter: sorption experiments and molecular dynamics simulation. Sci. Total Environ. 508, 276–287.
An, C.J., Huang, G.H., Yu, H., Wei, J., Chen, W., Li, G.C., 2010. Effect of short-chain organic acids and pH on the behaviors of pyrene in soil-water system. Chemosphere 81, 1423–1429.
Cao, Q.M., Wang, H., Qin, J.Q., Chen, G.Z., Zhang, Y.B., 2015. Partitioning of PAHs in pore water from mangrove wetlands in Shantou, China. Ecotoxicol. Environ. Saf. 11, 42–47.
Chen, Y., Lv, D., Li, X.H., Zhu, T.L., 2018. $PM_{2.5}$-bound phthalates in indoor and outdoor air in Beijing: seasonal distributions and human exposure via inhalation. Environ. Pollut. 241, 369–377.
Cheng, Z., Nie, X.P., Wang, M.H., 2013. Risk assessments of human exposure to bioaccessible phthalate esters through market fish consumption. Environ. Int. 57, 75–80.
Clarke, B.O., Smith, S.R., 2011. Review of 'emerging' organic contaminants in biosolids and assessment of international research priorities for the agricultural use of biosolids. Environ. Int. 37, 226–247.
Cornelissen, G., Gustafsson, O., Bucheli, T.D., Jonker, M.T.O., Koelmans, A.A., van Noort, P.C.M., 2005. Extensive sorption of organic compounds to black carbon, coal, and kerogen in sediments and soils: mechanisms and consequences for distribution, bioaccumulation, and biodegradation. Environ. Sci. Technol. 39, 6881–6895.
Fromme, H., Kuchler, T., Otto, T., Pilz, K., Muller, J., Wenzel, A., 2002. Occurrence of phthalates and bisphenol A and F in the environment. Water Res. 36, 1429–1438.
Gu, J.D., Li, J., Wang, Y., 2005. Biochemical pathway and degradation of phthalate ester isomers by bacteria. Water Sci. Technol. 52, 241–248.
Guo, Y., Wu, Q., Kannan, K., 2011. Phthalate metabolites in urine from China, and implications for human exposures. Environ. Int. 37, 893–898.
Haichar, F.E., Santaella, C., Heulin, T., Achouak, W., 2014. Root exudates mediated interactions below ground. Soil Biol. Biochem. 77, 69–80.
Jia, H., Hou, D.Y., Dai, M.Y., Lu, H.L., Yan, C.L., 2018. Effects of root exudates on the mobility of pyrene in mangrove sediment-water system. Catena 162, 396–401.
Kim, Y., Ha, E.H., Kim, E.J., Park, H., Ha, M., Kim, J.H., Hong, Y.C., Chang, N., Kim, B.N., 2011. Prenatal exposure to phthalates and infant development at 6 months: prospective mothers and children's environmental health (MOCEH) study. Environ. Health Perspect. 119, 1495–1500.
Li, T., Yin, P.H., Zhao, L., Wang, G.F., Yu, Q.J., Li, H., Duan, S., 2015. Spatial-temporal distribution of phthalate esters from riverine outlets of Pearl River Delta in China. Water Sci. Technol. 71, 183–190.
Lin, Z.-P., Ikonomou, M.G., Jing, H., Mackintosh, C., Gobas, F.A.P.C., 2003. Determination of phthalate ester congeners and mixtures by LC/ESI-MS in sediments and biota of an urbanized marine inlet. Environ. Sci. Technol. 37, 2100–2108.
Lin, Y.L., Wang, L., Li, R., Hu, S.B., Wang, Y.F., Xue, Y.W., Yu, H., Jiao, Y.Q., Wang, Y.H., Zhang, Y., 2018. How do root exudates of bok choy promote dibutyl phthalate adsorption on mollisol? Ecotoxicol. Environ. Saf. 161, 129–136.
Liu, H., Liang, H., Liang, Y., Zhang, D., Wang, C., Cai, H., Shvartsev, S.L., 2010. Distribution of phthalate esters in alluvial sediment: a case study at JiangHan plain, Central China. Chemosphere 78, 382–388.
Liu, H., Zhang, D., Li, M.J., Tong, L., Feng, L., 2013. Competitive adsorption and transport of phthalate esters in the clay layer of JiangHan plain, China. Chemosphere 92, 1542–1549.
Lopez-Sangil, L., Rovira, P., 2013. Sequential chemical extractions of the mineral-associated soil organic matter: an integrated approach for the fractionation of organo-mineral complexes. Soil Biol. Biochem. 62, 57–67.
Lu, H.L., Yan, C.L., Liu, J.C., 2007. Low-molecular-weight organic acids exuded by mangrove (*Kandelia candel* (L.) Druce) roots and their effect on cadmium species change in the rhizosphere. Environ. Exp. Bot. 61, 159–166.
Maraqa, M.A., Zhao, X., Lee, J.U., Allan, F., Voice, T.C., 2011. Comparison of nonideal sorption formulations in modeling the transport of phthalate esters through packed soil columns. J. Contam. Hydrol. 125, 57–69.

Mirmohamadsadeghi, S., Kaghazchi, T., Soleimani, M., Asasian, N., 2012. An efficient method for clay modification and its application for phenol removal from wastewater. Appl. Clay Sci. 59–60, 8–12.
Net, S., Sempere, R., Delmont, A., Paluselli, A., Ouddane, B., 2015. Occurrence, fate, behavior and ecotoxicological state of phthalates in different environmental matrices. Environ. Sci. Technol. 49, 4019–4035.
Paluselli, A., Aminot, Y., Galgani, F., Net, S., Sempéré, R., 2018. Occurrence of phthalate acid esters (PAEs) in the northwestern Mediterranean Sea and the Rhone River. Prog. Oceanogr. 163, 221–231.
Pan, Y., Chen, J., Zhou, H.C., Farzana, S., Tam, N.F.Y., 2017. Vertical distribution of dehalogenating bacteria in mangrove sediment and their potential to remove polybrominated diphenyl ether contamination. Mar. Pollut. Bull. 124, 1055–1062.
Réguer, A., Sochard, S., Hort, C., Platel, V., 2011. Measurement and modelling of adsorption equilibrium, adsorption kinetics and breakthrough curve of toluene at very low concentrations on to activated carbon. Environ. Technol. 32, 757–766.
Rinklebe, J., Shaheen, S.M., Schröter, F., Rennert, T., 2015. Exploiting biogeochemical and spectroscopic techniques to assess the geochemical distribution and release dynamics of chromium and lead in a contaminated floodplain soil. Chemosphere 150, 390–397.
Salapasidou, M., Samara, C., Voutsa, D., 2011. Endocrine disrupting compounds in the atmosphere of the urban area of Thessaloniki, Greece. Atmos. Environ. 45, 3720–3729.
Shukla, K.P., Sharma, S., Singh, N.K., Singh, V., Tiwari, K., Singh, S., 2011. Nature and role of root exudates: efficacy in bioremediation. Afr. J. Biotechnol. 10, 9717–9724.
Sun, H.F., Shi, J., Guo, S., Zhang, Y., Duan, L.S., 2016. *In situ* determination of the depuration of three- and four-ringed polycyclic aromatic hydrocarbons co-adsorbed onto mangrove leaf surfaces. Environ. Pollut. 208, 688–695.
Sun, K., Jin, J., Keiluweit, M., Kleber, M., Wang, Z.Y., Pan, Z.Z., Xing, B.S., 2012. Polar and aliphatic domains regulate sorption of phthalic acid esters (PAEs) to biochars. Bioresour. Technol. 118, 120–127.
Sun, K., Ro, K., Guo, M., Novak, J., Mashayekhi, H., Xing, B., 2011. Sorption of bisphenol A, 17[alpha]-ethinyl estradiol and phenanthrene on thermally and hydrothermally produced biochars. Bioresour. Technol. 102, 5757–5763.
Tao, S., Chen, Y.J., Xu, F.L., Cao, J., Li, B.G., 2003. Changes of copper speciation in maize rhizosphere soil. Environ. Pollut. 122, 447–454.
Vimonses, V., Lei, S.M., Jin, B., Chowd, C.W.K., Saint, C., 2009. Kinetic study and equilibrium isotherm analysis of Congo red adsorption by clay materials. Chem. Eng. J. 148, 354–364.
Wang, X.H., Zhao, K.Y., Yang, B.X., Chen, T., Li, D.Y., Wu, H., Wei, J.F., Wu, X.Q., 2016. Adsorption of dibutyl phthalate in aqueous solution by mesoporous calcium silicate grafted non-woven polypropylene. Chem. Eng. J. 306, 452–459.
Wang, Y.Y., Fang, L., Lin, L., Luan, T.G., Tam, N.F.Y., 2014. Effects of low molecular-weight organic acids and dehydrogenase activity in rhizosphere sediments of mangrove plants on phytoremediation of polycyclic aromatic hydrocarbons. Chemosphere 99, 152–159.
Wu, W., Sheng, H.J., Gu, C.G., Song, Y., Willbold, S., Qiao, Y., Liu, G.X., Zhao, W., Wang, Y., Jiang, X., Wang, F., 2018. Extraneous dissolved organic matter enhanced adsorption of dibutyl phthalate in soils: insights from kinetics and isotherms. Sci. Total Environ. 631–632, 1495–1503.
Xu, X.R., Li, X.Y., 2008. Adsorption behaviour of dibutyl phthalate on marine sediments. Mar. Pollut. Bull. 57, 403–408.
Yuan, S.Y., Huang, I.C., Chang, B.V., 2010. Biodegradation of dibutyl phthalate and di-(2-ethylhexyl) phthalate and microbial community changes in mangrove sediment. J. Hazard. Mater. 184, 826–831.
Zeng, F., Wen, J.X., Cui, K.Y., Wu, L.N., Liu, M., Li, Y.J., Lin, Y.J., Zhu, F., Ma, Z.L., Zeng, Z.X., 2009. Seasonal distribution of phthalate esters in surface water of the urban lakes in the subtropical city, Guangzhou, China. J. Hazard. Mater. 169, 719–725.
Zhang, W.M., Xu, Z.W., Pan, B.C., Hong, C.H., Jia, K., Jiang, P.J., Zhang, Q.J., Pan, B.J., 2008. Equilibrium and heat of adsorption of diethyl phthalate on heterogeneous adsorbents. J. Colloid Interface Sci. 325, 41–47.
Zhao, J., Ji, Y.Q., Zhu, Z.Y., Zhang, W., Zhang, L., Zhao, J.B., 2018. PAEs occurrence and sources in road dust and soil in/around parks in May in Tianjin, China. Ecotoxicol. Environ. Saf. 147, 238–244.